© 2015. Published by The Company of Biologists Ltd | Development (2015) 142, 2641-2652 doi:10.1242/dev.126318

RESEARCH ARTICLE

Evf2 lncRNA/BRG1/DLX1 interactions reveal RNA-dependent inhibition of chromatin remodeling

Ivelisse Cajigas[1], David E. Leib[1,*], Jesse Cochrane[2], Hao Luo[1], Kelsey R. Swyter[1], Sean Chen[1,‡], Brian S. Clark[1,§], James Thompson[3], John R. Yates, III[3], Robert E. Kingston[2] and Jhumku D. Kohtz[1,¶]

ABSTRACT

Transcription-regulating long non-coding RNAs (lncRNAs) have the potential to control the site-specific expression of thousands of target genes. Previously, we showed that *Evf2*, the first described ultraconserved lncRNA, increases the association of transcriptional activators (DLX homeodomain proteins) with key DNA enhancers but represses gene expression. In this report, mass spectrometry shows that the *Evf2*-DLX1 ribonucleoprotein (RNP) contains the SWI/SNF-related chromatin remodelers Brahma-related gene 1 (BRG1, SMARCA4) and Brahma-associated factor (BAF170, SMARCC2) in the developing mouse forebrain. *Evf2* RNA colocalizes with BRG1 in nuclear clouds and increases BRG1 association with key DNA regulatory enhancers in the developing forebrain. While BRG1 directly interacts with DLX1 and *Evf2* through distinct binding sites, *Evf2* directly inhibits BRG1 ATPase and chromatin remodeling activities. *In vitro* studies show that both RNA-BRG1 binding and RNA inhibition of BRG1 ATPase/remodeling activity are promiscuous, suggesting that context is a crucial factor in RNA-dependent chromatin remodeling inhibition. Together, these experiments support a model in which RNAs convert an active enhancer to a repressed enhancer by directly inhibiting chromatin remodeling activity, and address the apparent paradox of RNA-mediated stabilization of transcriptional activators at enhancers with a repressive outcome. The importance of BRG1/RNA and BRG1/homeodomain interactions in neurodevelopmental disorders is underscored by the finding that mutations in Coffin–Siris syndrome, a human intellectual disability disorder, localize to the BRG1 RNA-binding and DLX1-binding domains.

KEY WORDS: Long non-coding RNA, Chromatin remodeling, Homeodomain proteins, *Evf2*, *Dlx6os1*, BRG1, SMARCA4

INTRODUCTION

Genome-wide studies revealed that the majority of RNA transcripts in mammalian cells do not encode proteins [non-coding RNAs (ncRNAs)]. Long non-coding RNAs (lncRNAs) have emerged as a class of molecules with highly diverse structures and functions, including roles in transcriptional regulation (Geisler and Coller, 2013; Yang et al., 2014). Reports of single *trans*-acting lncRNAs controlling gene expression in cell lines (Lanz et al., 1999; Feng et al., 2006; Rinn et al., 2007) or in mice (Bond et al., 2009; Gabory et al., 2009; Rapicavoli et al., 2011) have been expanded by the genomic era to include thousands of lncRNAs with the potential for transcriptional effects. Families of enhancer RNAs (eRNAs; Ørom et al., 2010), ultraconserved RNAs [ucRNAs; also known as transcribed ultraconserved RNAs (t-UCRs); Calin et al., 2007] and opposite strand transcripts [OS; also called natural antisense transcripts (NATs); Yelin et al., 2003] have been identified. The biological significance of lncRNAs has increased with reports of roles in disease processes as diverse as lung cancer (Gutschner et al., 2013), pain response (Zhao et al., 2013) and microbial susceptibility (Gomez et al., 2013).

Transcription-regulating lncRNAs are not only functionally but also mechanistically diverse, regulating gene expression through *trans* and *cis* effects. Studies on *Evf2*, the first lncRNA member of larger classes of ucRNAs/t-UCRs, show that *Evf2* (*Dlx6os1*, *Dlx6as*) is transcribed on the opposite strand, antisense to *Dlx6*, and therefore also belongs to the class of OS/NATs (Feng et al., 2006). Although antisense transcription predicted that *Evf2* would have *cis*-regulatory effects, multiple experiments suggest that *Evf2* exhibits both *trans* and *cis* effects (Feng et al., 2006; Bond et al., 2009; Berghoff et al., 2013). Chromatin immunoprecipitation (ChIP) experiments show that *Evf2* increases the binding of transcriptional activators (DLX1/2; Zerucha et al., 2000) and the repressor methyl-CpG binding protein 2 (MECP2; Nan et al., 1997) to key *Dlx5/6* enhancers (Zerucha et al., 2000) with a repressive outcome (Bond et al., 2009). Genetic epistasis experiments support a model in which *Evf2* regulates *Dlx5/6* gene expression by modulating the antagonistic interactions between DLX1/2 and MECP2, and regulating *Dlx5/6* ultraconserved enhancer site-specific methylation (Berghoff et al., 2013). However, beyond complex formation with DLX proteins, *Evf2*-ribonucleoprotein (RNP)-containing complexes have not been characterized.

In these studies, we further investigate the mechanism of *Evf2* transcriptional control, and focus on mouse E13.5 ganglionic eminence (GE), the site of sonic hedgehog activation of *Dlx1/2/5/6* and *Evf2* gene expression (Kohtz et al., 1998; Feng et al., 2006). Using mass spectrometry to sequence *Evf2*/DLX RNP complexes *in vivo*, we identify direct interactions between *Evf2* and BRG1/BAFs, which are components of a SWI/SNF-related chromatin remodeling complex (Wang et al., 1996; Phelan et al., 1999; Kasten et al., 2011; Staahl and Crabtree, 2013), and between BRG1 (SMARCA4) and the DLX1 homeodomain protein. While *Evf2* increases the association of BRG1 with key *Dlx5/6* DNA regulatory enhancers in the developing forebrain, *Evf2* also inhibits BRG1 ATPase and chromatin remodeling activity *in vitro*. *Evf2*/BRG1, *Evf2*-BAF170 (SMARCC2), and *Evf2*-BAF155 (SMARCC1) interactions are competed by specific ribohomopolymers but not tRNA, suggesting

[1]Developmental Biology and Department of Pediatrics, Stanley Manne Children's Research Institute and Feinberg School of Medicine, Northwestern University, Box 204, 2430 N. Halsted, Chicago, IL 60614, USA. [2]Department of Molecular Biology, Harvard University, Boston, MA 02114, USA. [3]The Scripps Research Institute, La Jolla, CA 92037, USA.
*Present address: Department of Neuroscience, UC San Francisco, CA 94143, USA. ‡Present address: Department of Molecular Biology, UC Berkeley, CA 94720, USA. §Present address: Department of Neuroscience, Johns Hopkins University, Baltimore, MD 21218, USA.

¶Author for correspondence (j-kohtz@northwestern.edu)

Received 9 May 2015; Accepted 9 June 2015

Development (2015) 142, 2641-2652 doi:10.1242/dev.126318

that RNA structure and length, but not sequence complexity, determine RNA binding. Together, these data support the contention that lncRNA-mediated transcriptional repression occurs through direct inhibition of chromatin remodeling, a mechanism distinct from recruitment of histone modification enzymes (Rinn et al., 2007; Nagano et al., 2008; Pandey et al., 2008; Zhao et al., 2008). Given that the BRG1 RNA-binding domain and one of the BRG1 DLX1-binding domains are mutated in the human intellectual disorder Coffin–Siris syndrome (CSS; Tsurusaki et al., 2012, 2014), characterization of RNA-mediated chromatin remodeling might be important for understanding neurodevelopmental disorders.

RESULTS

Evf2/DLX1 complexes contain SWI/SNF-related chromatin remodelers

Previous results show that *Evf2* forms nuclear complexes with DLX homeodomain proteins (Feng et al., 2006) and that association of DLX1/2 with key *Dlx5/6* DNA regulatory sequences decreases in mice lacking *Evf2* (*Evf2*$^{TS/TS}$) (Bond et al., 2009). *Evf2*$^{TS/TS}$ mice were generated by insertion of a triple polyA transcription STOP sequence (TS) in the 5′ end of *Evf2*, successfully preventing *Evf2* transcription without disrupting expression of the adjacent *Evf1* transcript (Bond et al., 2009). As described above, the E13.5 mouse GE is the site of sonic hedgehog-induced *Dlx1/2/5/6* and *Evf1/2* activation during forebrain development (Kohtz et al., 1998, 2001; Feng et al., 2006). In order to study *Evf2* RNA/DLX protein complexes in E13.5 GE, we used anti-DLX immunoaffinity purification followed by mass spectrometry sequencing. We cross-linked a well-characterized anti-pan-DLX antibody (Kohtz et al., 2001; Feng et al., 2004, 2006; Bond et al., 2009) to cyanogen bromide-activated Sepharose beads, purified complexes from wild-type (*Evf2*$^{+/+}$) and *Evf2*$^{TS/TS}$ E13.5 GE nuclear extracts, and compared the identity of DLX-bound proteins in the presence and absence of *Evf2* RNA by mass spectrometry sequencing (Washburn et al., 2001).

DLX1 is the only DLX family member identified in both *Evf2*$^{+/+}$ and *Evf2*$^{TS/TS}$ extracts. Members of SWI/SNF-related chromatin remodeling complexes are identified in *Evf2*$^{+/+}$ nuclear extracts (Fig. 1A). DLX1-bound complexes from *Evf2*$^{+/+}$ nuclear extracts contain the following eight proteins with the potential to affect chromatin remodeling: BRG1, BAF170, ARID1A (predicted), SNF2L (SMARCA1) and SNF2H (SMARCA5) (mammalian ISWI homologs), BAZ1A and BAZ1B (bromodomain adjacent to zinc finger proteins) and polybromo 1 (for a complete list of proteins see supplementary material Table S1). Total BRG1 and BAF170 protein levels are the same in *Evf2*$^{+/+}$ and *Evf2*$^{TS/TS}$ nuclear extracts (Fig. 1B), supporting that mass spectrometry differences in BRG1 and BAF170 from *Evf2*$^{+/+}$ and *Evf2*$^{TS/TS}$ DLX complexes do not result from *Evf2* regulation of BRG1 or BAF170 protein production or stability. The endogenous DLX1-BRG1 complex in *Evf2*$^{+/+}$ E13.5 GE nuclear extracts is further confirmed by co-immunoprecipitation of BRG1 with anti-DLX antibody (Fig. 1C). Although immunoprecipitation is performed in the presence of protease inhibitors, BRG1 might be cleaved during the immunoprecipitation process, as multiple bands are detected after immunoprecipitation with anti-BRG1 and anti-DLX (Fig. 1C).

BRG1 is an essential component of SWI/SNF-related chromatin remodeling complexes that contain different combinations of BAFs, depending on cell type and state of differentiation (Lessard et al., 2007). BRG1 is an ATPase that can remodel nucleosome positioning along the DNA, even in the absence of other BAFs, *in vitro* (Workman and Kingston, 1992; Phelan et al., 1999). BRG1-BAFs regulate gene expression crucial for neural progenitor differentiation (Lessard et al., 2007; Yoo and Crabtree, 2009). In addition, *Brg1* null mice show decreased *Dlx1* gene expression in the developing ventral telencephalon (Lessard et al., 2007). These studies support a biological role of BRG1 in regulating gene expression in embryonic ventral telencephalic interneuron precursors, and led to further analysis of DLX-BRG1 complexes in E13.5 GE.

Protein complexes identified in nuclear extract lysates represent soluble but not necessarily chromatin-bound complexes. Given our previous experiments showing that *Evf2* increases DLX binding to *Dlx5/6* enhancers ei and eii (Bond et al., 2009), we next tested whether DLX-bound *Dlx5/6* ei and eii complexes also contain BRG1. We performed ChIP using anti-DLX, followed by elution, and then reChIP with anti-BRG1 (Fig. 1D). DLX-BRG1 co-complexes are detected at the ultraconserved *Dlx5/6* ei enhancer (site 2, but not sites 1 or 3; Fig. 1D). The ability to detect DLX-BRG1 complexes at *Dlx5/6* ei but not eii could be due to differences in DLX and BRG1 enrichment at ei and eii, combined with the low efficiency of reChIP. Together, these data support the presence of both soluble and enhancer-bound DLX1-BRG1 complexes in E13.5 GE. The presence of DLX-BRG1 complexes at the *Dlx5/6* ei enhancer supports a functional role for BRG1 in regulating enhancer activity.

BRG1 colocalizes with *Evf2* RNA clouds

Fluorescent RNA *in situ* hybridization (FISH) previously showed that *Evf2* forms nuclear RNA clouds in E13.5 GE neuronal progenitors, colocalizing with DLX homeodomain proteins (Feng et al., 2006). *Evf2* RNA clouds appear similar to those reported for lncRNAs involved in imprinting, namely *Xist* and *Kcnq1ot1* (Redrup et al., 2009; Brockdorff, 2011). Fluorescent RNA *in situ* hybridization and immunolocalization (FISH-immuno), followed by confocal microscopy, shows that BRG1 colocalizes with *Evf2* in E13.5 GE nuclear RNA clouds (Fig. 1E-F″). Confocal *z*-stack analysis shows that BRG1 is scattered within the *Evf2* RNA cloud (Fig. 1F). Intensity plots show enrichment of BRG1 within *Evf2* clouds for the majority of nuclei (21/25) expressing *Evf2* (Fig. 1G; supplementary material Fig. S1). This supports the idea that *Evf2*-BRG1 interactions occur within RNA clouds, but also suggests that there is heterogeneity in the relative distribution of *Evf2* and BRG1 among E13.5 GE interneuron precursors.

BRG1 contains two distinct DLX1-binding domains that correspond to sites of mutations found in CSS and overlap with the SNF2 ATP-coupling domain

Isolation of DLX1 complexes containing BRG1/BAF170 raises the possibility of direct interactions between DLX1 and BRG1/BAF170. Co-immunoprecipitation experiments using Flag-tagged BRG1 (Fig. 2A) and His-tagged DLX1 indicate that BRG1 directly binds DLX1, but not the control His-tagged protein SODb (Fig. 2B). In addition, BAF47 (SMARCB1; Wang et al., 1996), but not BAF170 or BAF155 (low-intensity band) bind DLX1 (Fig. 2C). Mass spectrometry results identified DLX1-BRG1 complexes in nuclear extracts containing *Evf2* (*Evf2*$^{+/+}$) but not in its absence (*Evf2*$^{TS/TS}$) (Fig. 1A), raising the possibility that DLX1-BRG1 interactions might result from direct or indirect effects of *Evf2*. However, direct interactions between DLX1 and BRG1 in the absence of *Evf2* (Fig. 2B) show that DLX1-BRG1 binding does not require the presence of *Evf2 in vitro*. Because we are dealing with such small amounts of protein (derived from embryonic brain GE

Development (2015) 142, 2641-2652 doi:10.1242/dev.126318

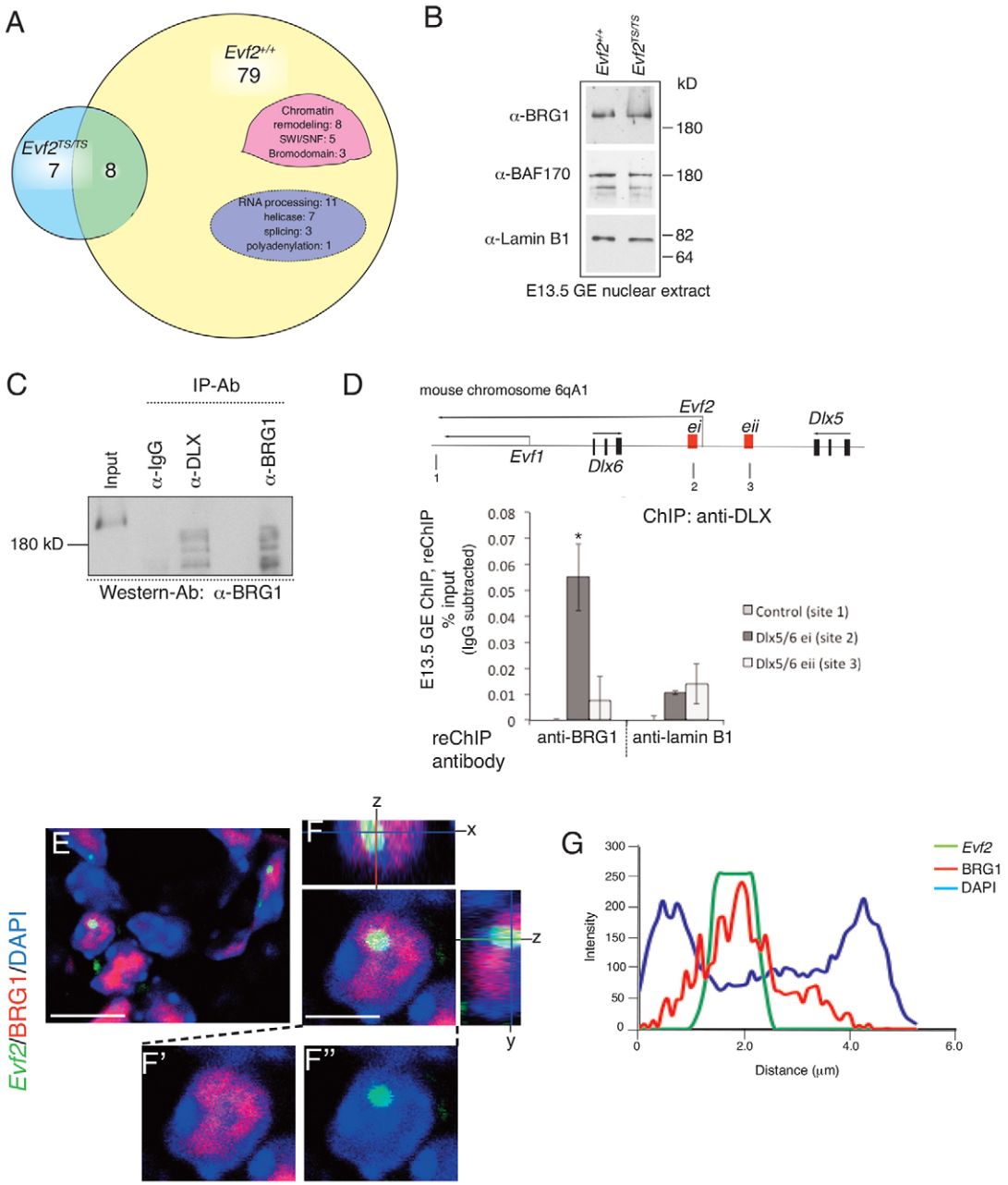

Fig. 1. Identification of *Evf2*/DLX1/BRG1 complexes in mouse embryonic brain. (A) Venn diagram summarizing the results from mass spectrometry sequencing of E13.5 ganglionic eminence (GE) brain protein complexes. Proteins from E13.5 GE nuclear extracts were affinity purified on an anti-DLX column and sequenced. Among a total of 87 $Evf2^{+/+}$ proteins, 79 were unique to $Evf2^{+/+}$, of which eight were associated with CRs and 11 with RNA processing. Among a total of 15 $Evf2^{TS/TS}$ proteins, seven were unique to $Evf2^{TS/TS}$. Eight proteins were common to $Evf2^{+/+}$ and $Evf2^{TS/TS}$. (B) Western blot analysis of $Evf2^{+/+}$ and $Evf2^{TS/TS}$ nuclear extracts shows equal amounts of BRG1, BAF170 and lamin B proteins. (C) Co-immunoprecipitation of DLX/BRG1 complexes from $Evf2^{+/+}$ E13.5 GE nuclear extracts. Immunoprecipitation with the antibodies indicated (IP-Ab) was followed by western blot analysis and probing with anti-BRG1 antibody. Input (10%) is loaded in the first lane; 25% of the anti-BRG1 immunoprecipitated protein is loaded in the last lane. (D) ChIP, followed by reChIP, defines a co-complex of DLX/BRG1 localized to the *Dlx5/6* ultraconserved enhancer (ei). E13.5 GE chromatin was immunoprecipitated first with anti-DLX, and eluted complexes were then immunoprecipitated with anti-BRG1, anti-lamin B or anti-IgG. Percent input values are obtained after subtraction of IgG values. Primer sites (1-3) are indicated in the schematic. *$P<0.05$ (Student's two-tailed *t*-test) for BRG1, but not lamin B. Error bars indicate s.e.m. Chromatin was isolated from a pool of ~20 GEs, and experiments were duplicated. (E-F″) Visualization of RNA/protein clouds in E13.5 GE. *Evf2* fluorescent RNA *in situ* hybridization (FISH; green) and immunofluorescent detection of BRG1 protein (red) are visualized by confocal microscopy. Nuclei are stained with DAPI (blue). Confocal *z*-stack images show *Evf2*/BRG1 colocalization in yellow. (G) Fluorescent intensity profiles across the nucleus of a neuronal precursor in E13.5 GE (*Evf2* RNA, green; BRG1 protein, red; nuclei, blue). In this nucleus, the highest peaks from *Evf2* and BRG1 coincide, showing enrichment. Additional scans are shown in supplementary material Fig. S1, indicating *Evf2*/BRG1 correlation in the majority of nuclei, as well as some heterogeneity. Scale bars: 10 μm in E; 4 μm in F.

nuclear extract lysates), we predict that the mass spectrometry results reflect enrichment rather than absolute numbers. Therefore, the mass spectrometry data indicating that BRG1 bound to DLX1 is detected in $Evf2^{+/+}$, but not $Evf2^{TS/TS}$, supports enrichment in the presence of *Evf2* but does not exclude the possibility that some amount of BRG1 is bound to DLX1 in $Evf2^{TS/TS}$. Together, these

Development (2015) 142, 2641-2652 doi:10.1242/dev.126318

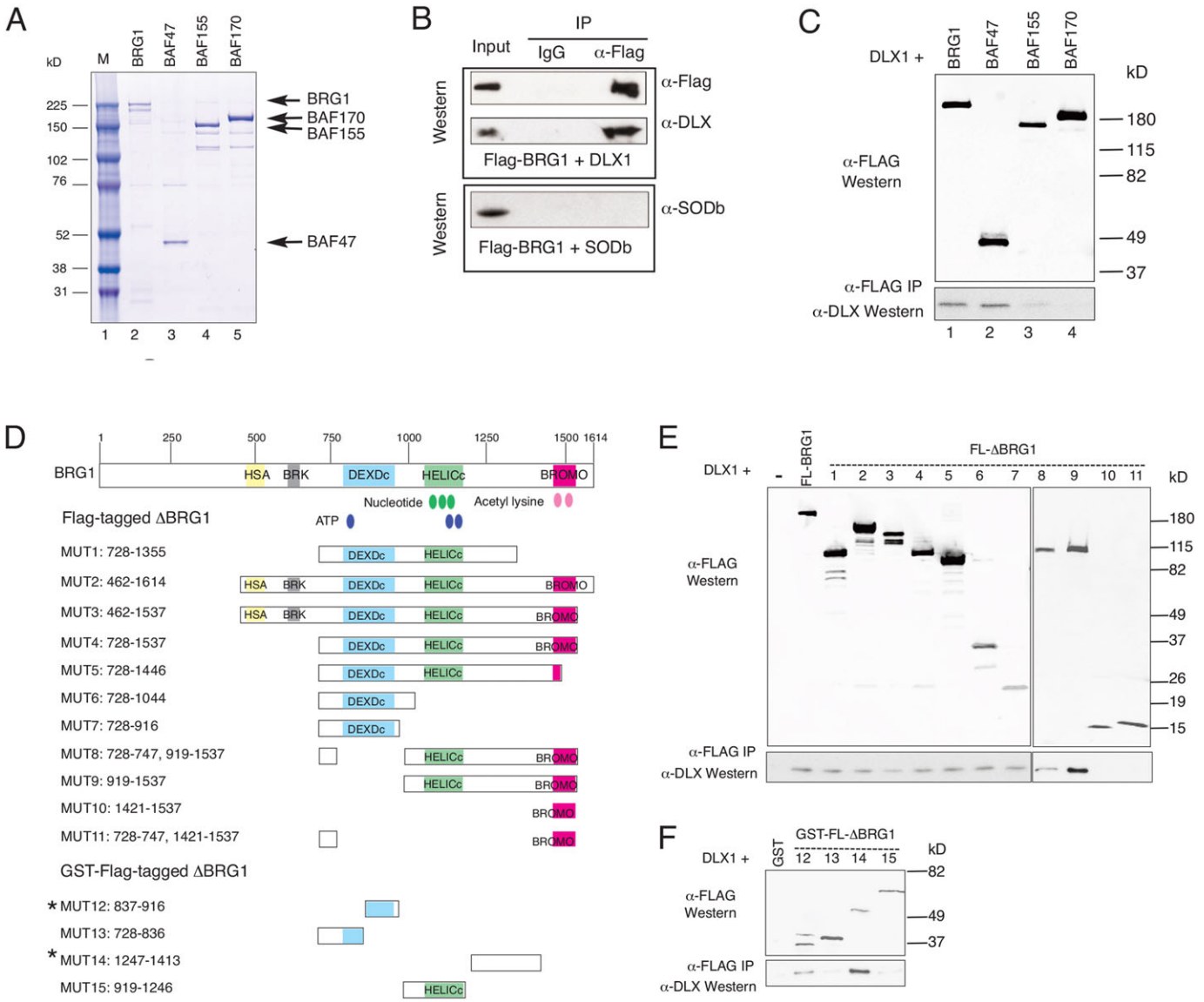

Fig. 2. BRG1 binds DLX1 through two distinct binding domains. (A) Coomassie stain of Flag-tagged proteins isolated from baculovirus-infected insect cells. M, prestained size marker. (B-F) Direct interactions between DLX1 and BRG1 or BAF47. Flag-tagged and GST recombinant fusion proteins (8 pmoles) were: BRG1, FL-Δ-BRG1 (MUT1-15), BAF47, BAF155 and BAF170. His-tagged proteins (14 pmoles) were: DLX1, SODb. (B) DLX1 and BRG1 direct interactions. Flag-BRG1 is incubated with His-tagged DLX1 or His-tagged SODb, and immunoprecipitated (IP) with anti-IgG or anti-Flag-conjugated agarose. Western blot of IP complexes with anti-Flag, anti-DLX or anti-SODb indicates that DLX1 directly binds to BRG1. (C) DLX1 directly interacts with BAF47, but not BAF155 or BAF170. His-tagged DLX1 is incubated with Flag-tagged proteins, immunoprecipitated with anti-Flag and probed with anti-DLX by western blot. (D) Schematic of Flag-tagged BRG1 recombinant proteins. MUT 12-14 are GST fusions. Known functional domains include nucleotide-, ATP- and acetyl lysine-binding domains (green, blue and pink ovals) and HSA (helicase/SANT associated, β-actin binding), BRK (chromodomain/helicase shared domain with unknown function), DEXDc (DEAD-like helicase), HELICc (helicase) and BROMO (bromodomain). (E,F) Co-immunoprecipitation experiments with DLX1 and Flag-tagged BRG1 FL-Δ-BRG1 MUT1-15; anti-Flag detects BRG1 input, while anti-DLX1 detects DLX1 protein bound to BRG1.

data support the formation of DLX1-BRG1-BAF170 complexes, stabilized by direct interactions between DLX1 and BRG1, and DLX1 and BAF47.

In order to define further the mechanism of BRG1-DLX1 interactions, we performed co-immunoprecipitation experiments with recombinant DLX1 and BRG1 deletion mutants (Fig. 2D-F). Two regions of BRG1 are sufficient to bind DLX1 [BRG1 837-916 (MUT12) and 1247-1413 (MUT14)]. BRG1 DLX1-binding domain 1 (837-916) localizes to a region known to contain mutations in CSS (Tsurusaki et al., 2012, 2014); BRG1 DLX1-binding domain 2 (1247-1413) is highly conserved and overlaps the SNF2 ATP-coupling domain (SnAC; see Fig. 6A), a region known to be required for yeast SNF2 remodeling and histone binding (Sen et al., 2013). Thus, DLX1-BRG1 interactions have the potential to play a role in a neurodevelopmental disorder.

Evf2 increases BRG1 binding to key *Dlx5/6* enhancers with changes in histone H3 and H4 lysine acetylation

Previous results show that *Evf2* increases the association of DLX1/2 with the *Dlx5/6* ei and eii intergenic enhancers (Bond et al., 2009). We next used ChIP to determine whether *Evf2* affects BRG1 binding in the *Dlx5/6* region. E13.5 GE chromatin from *Evf2*$^{+/+}$ and *Evf2*$^{TS/TS}$ were compared for BRG1 occupancy (Fig. 3B). In the absence of *Evf2*, BRG1 binding to *Dlx5/6* ei and eii decreases.

Development (2015) 142, 2641-2652 doi:10.1242/dev.126318

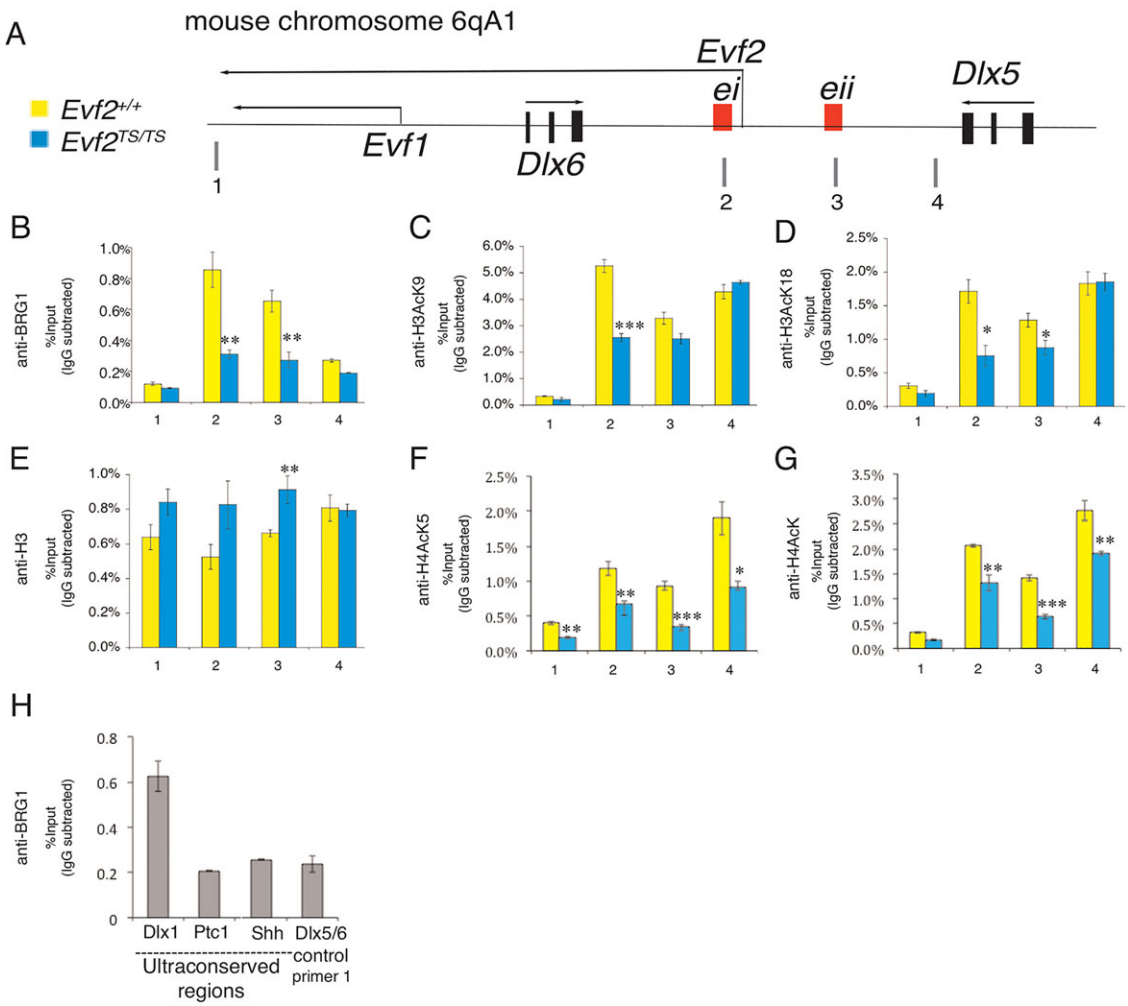

Fig. 3. *Evf2* stabilizes BRG1 binding to key DNA regulatory enhancers in the *Dlx5/6* intergenic region. (A) Mouse chromosome 6qA1 (*Dlx5/6* region) showing relative location of q-PCR primers (1-4), *Dlx5/6* enhancers (the ultraconserved enhancer ei and the conserved enhancer eii, red boxes) and *Evf2*, *Evf1*, *Dlx5*, *Dlx6* transcripts (black arrows). Dlx5 and Dlx6 protein coding exons (black boxes). (B-G) ChIP of $Evf2^{+/+}$ (yellow bars) and $Evf2^{TS/TS}$ (blue bars) E13.5 GE tissue is followed by q-PCR using primers at sites 1-4. Antibodies for ChIP are indicated on the *y*-axis. Primer 1, a site downstream of the 3′ end of *Evf2*; primers 2-4 are *Dlx5/6* intergenic sites: primer 2, ei; primer 3, eii (Zerucha et al., 2000); primer 4, an adjacent intergenic region with no known regulatory role. **P*<0.05, ***P*<0.01, ****P*<0.001 (Student's two-tailed *t*-test), *n*=10 embryos each genotype; error bars indicate s.e.m. (H) Anti-BRG1 ChIP from E13.5 GE. q-PCR shows enrichment of BRG1 at a subset of UCR sites: the *Dlx1* UCR site, but not the *Ptc1* or *Shh* UCRs.

BRG1 binding to site 1 (located downstream of *Evf1*), representing the background level of BRG1 binding, and to site 4 (a *Dlx5/6* intergenic site) remain unaffected. Given the known interaction of the BRG1 bromodomain with acetylated lysines (Hassan et al., 2002), we next compared $Evf2^{+/+}$ and $Evf2^{TS/TS}$ chromatin for the levels of histone lysine acetylation in the *Dlx5/6* intergenic enhancers. ChIP using site-specific anti-H3 acetylated lysine antibodies on $Evf2^{TS/TS}$ E13.5 GE shows that H3AcK9 (Fig. 3C) and H3AcK18 (Fig. 3D) are significantly reduced at ei, and H3AcK18 to a lesser extent at eii, when compared with $Evf2^{+/+}$. Decreased H3 lysine acetylation is not a result of decreased nucleosome density, as total H3 does not decrease at ei or eii (Fig. 3E). In $Evf2^{TS/TS}$ chromatin, H4AcK5 decreases at four sites (Fig. 3F), while total H4AcK (Fig. 3G) decreases at three intergenic sites (sites 2-4).

We next asked whether BRG1 binds to other transcribed ultraconserved regions in E13.5 GE. Using the ultraconserved region (UCR) database (Woolfe et al., 2005), which reported over 1300 mouse UCRs, we searched for ucRNAs expressed in the developing brain (supplementary material Table S2). We identified three ucRNAs (*Dlx1UR*, *Ptc1UR* and *ShhUR*; supplementary material Fig. S2) that are expressed in E13.5 GE and transcribed on the opposite strand of genes in the SHH pathway (Marigo et al., 1996; Stone et al., 1996; Kohtz et al., 1998; Kohtz and Berghoff, 2010). ChIP shows that BRG1 is enriched in the *Dlx1* UCR, but not in the *Ptc1* (*Ptch1*) or *Shh* UCRs (Fig. 3H), supporting the idea that BRG1 binds a subset of transcribed UCRs *in vivo*.

Promiscuous binding of RNAs to BRG1

We previously reported that *Evf2* forms a complex with DLX proteins in nuclear clouds, in a soluble RNP from nuclear extracts, and increases DLX association with *Dlx5/6* ei and eii (Feng et al., 2006; Bond et al., 2009). However, direct interactions between *Evf2* RNA and DLX protein were not detected, suggesting involvement of an unknown RNA-binding protein. Complexes of DLX1 and BRG1 *in vivo*, direct interactions between DLX1 and BRG1 *in vitro*, and association between *Evf2* and BRG1 in RNA clouds led us to test whether BRG1 directly binds *Evf2*. RNA electrophoretic mobility shift assays (REMSAs) show that recombinant BRG1 directly binds *Evf2* (Fig. 4A). The *Evf2*

Development (2015) 142, 2641-2652 doi:10.1242/dev.126318

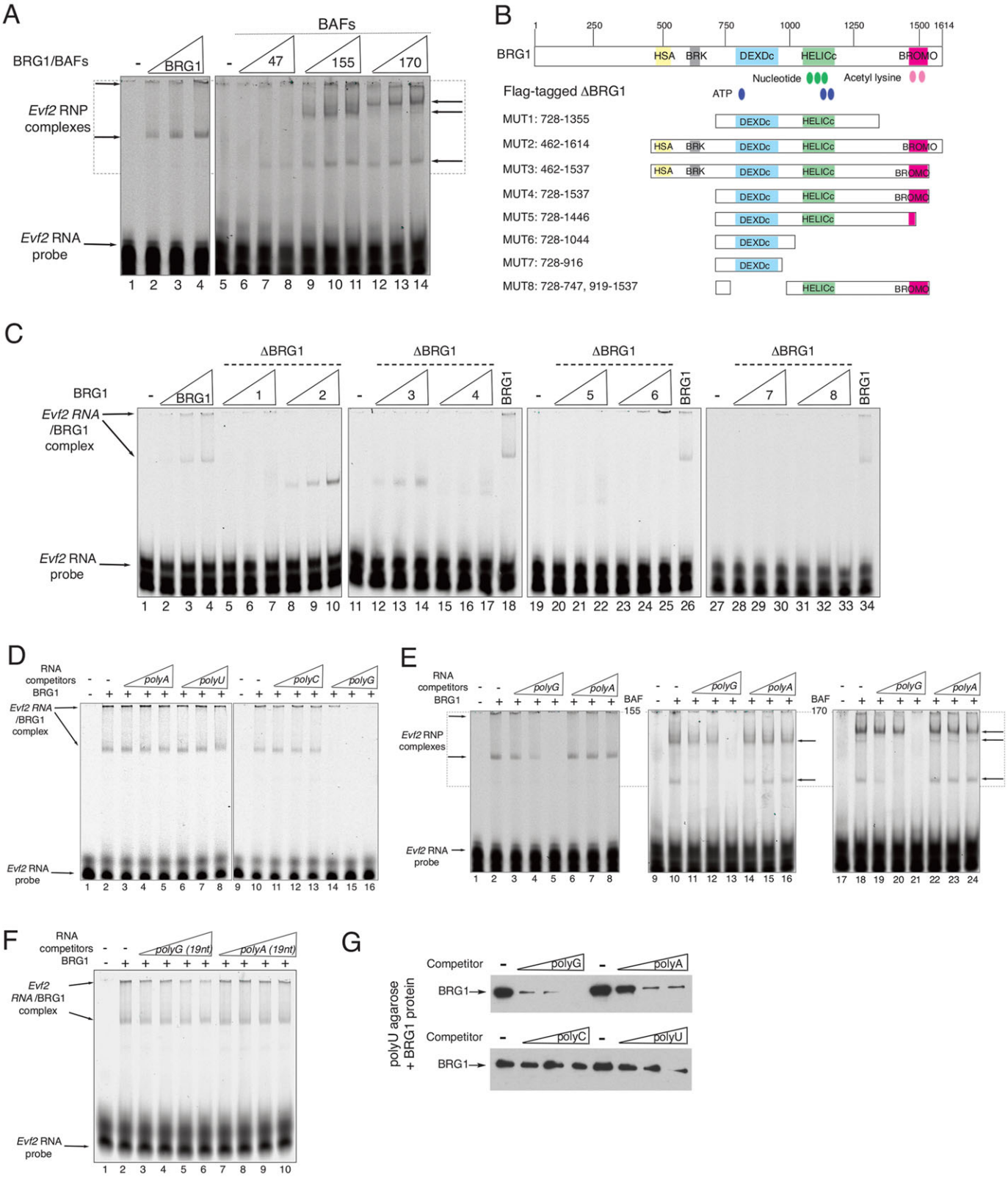

Fig. 4. See next page for legend.

RNA probe in REMSAs contains 115 bases spanning the *Evf2* UCR (blue boxed region in supplementary material Fig. S3A), a subregion of the *Evf2* transcription-regulating region (red boxed region in supplementary material Fig. S3A) as previously defined by Feng et al. (2006).

We next examined whether other members of the SWI/SNF complex bind *Evf2* RNA. We find that BAF155 and BAF170, but not BAF47, directly bind *Evf2* (Fig. 4A). We then used BRG1 deletion mutants to define the RNA-binding domain (RBD) in BRG1 to a region (462-728) containing the HSA and BRK domains (Fig. 4B,C).

Development (2015) 142, 2641-2652 doi:10.1242/dev.126318

Fig. 4. Characterization of direct interactions between *Evf2* RNA and BRG1/BAFs reveals promiscuous binding. RNA electrophoretic mobility shift assays (REMSAs) using near-infrared (NIR)-labeled *Evf2* RNA (ultraconserved sequence; supplementary material Fig. S3, blue dashed box) and recombinant Flag-tagged BRG1 and BAF proteins. (A) *Evf2* RNA probe (0.15 pmoles) is loaded in each lane with increasing concentrations of proteins: 2, 4, 8 picomoles; –, probe alone. (B) Flag-tagged BRG1 mutant proteins tested for binding to *Evf2* by REMSA in C. (C) Lanes 1-34 contain *Evf2* RNA probe with FL-BRG1 or FL-Δ-BRG1 (MUT1-8) added in increasing concentrations: 0.25, 1, 4 picomoles. (D) *Evf2* RNA and BRG1 complexes are incubated with unlabeled ribohomopolymers in increasing concentrations (0.625, 2.5, 10 µg) in competitive REMSAs. All lanes contain NIR-labeled *Evf2* RNA probe. BRG1 is added at 8 picomoles. (E) BRG1 (lanes 1-8), BAF155 (lanes 9-16) and BAF170 (lanes 17-24) complexes are incubated with unlabeled ribohomopolymers in increasing concentrations (0.008, 0.03, 0.125 µg) in competitive REMSAs. All lanes contain NIR-labeled *Evf2* RNA probe. BRG1, BAF155 or BAF170 is added at 8 picomoles. (F) *Evf2* RNA and BRG1 complexes are incubated with unlabeled ribohomopolymers (19 nt) in increasing concentrations (3.75, 7.5, 15.0, 30.0 picomoles) in competitive REMSAs. All lanes contain NIR-labeled *Evf2* RNA probe. BRG1 is added at 8 picomoles. (G) Ribohomopolymer competition in BRG1-polyU-agarose binding assays. Western blot analysis is shown of BRG1 bound to polyU-agarose. BRG1 recombinant protein is incubated with polyU-agarose in the absence of RNA competitor (–), and in the presence of increasing amounts (0.008, 0.03, 0.125 µg) of $polyG^{200\text{-}500nt}$, $polyA^{200\text{-}500nt}$, $polyC^{200\text{-}500nt}$ or $polyU^{200\text{-}500nt}$. Ribohomopolymer binding from highest to lowest affinity: polyG>polyA>polyU>polyC.

In order to determine the sequence specificity of *Evf2* RNA-BRG1 binding, we used ribohomopolymers in competitive REMSAs with *Evf2* and BRG1, BAF155 or BAF170 (Fig. 4D-F). *Evf2*-BRG1 interactions can be competed by polyG RNA, but not polyA, polyU or polyC RNAs (Fig. 4D). Similarly, *Evf2*-BAF170 (Fig. 4E) and *Evf2*-BAF155 interactions can be competed by $polyG^{200\text{-}500nt}$ but not $polyA^{200\text{-}500nt}$ RNA. Shorter $polyG^{19nt}$ cannot compete for *Evf2*-binding sites in BRG1 (Fig. 4F). The range of concentrations tested for $polyG^{200\text{-}500nt}$ is 0.05-146 picomoles (Fig. 4D,E), and the lowest competing concentration is 0.18-0.44 pmoles (Fig. 4E, lane 4). Even at the highest concentration of $polyG^{19nt}$ tested (30 pmoles; Fig. 4F, lane 6), it does not compete.

In order to test whether BRG1 binds directly to other ribohomopolymers, we performed ribohomopolymer competitions in BRG1/polyU-agarose binding assays (Fig. 4G). BRG1 directly binds polyU-agarose (– competitor lanes); polyG, polyA and polyU RNAs, but not polyC RNA, compete for BRG1 binding to polyU-agarose. In order to further characterize the RNA binding properties of BRG1, we tested BRG1 binding to the following sequence complex RNAs: artificial *pGEM* RNA transcript, *Dlx1UR* and *28S* RNA. All three RNAs outcompete *Evf2*-BRG1 binding (supplementary material Fig. S3B). Together, these data suggest that RNA binding by BRG1 is promiscuous, as it binds a subset of ribohomopolymers of a particular minimum length.

RNA inhibition of BRG1 ATPase activity and chromatin remodeling activity *in vitro*

In vitro chromatin remodeling assays show that the SWI/SNF-related chromatin remodelers displace purified nucleosomes on a DNA template (Workman and Kingston, 1992; Phelan et al., 1999; Whitehouse et al., 1999). The ATPase subunit BRG1 is sufficient to displace nucleosomes *in vitro*. Direct interactions between BRG1, BAF170 and BAF155 and RNAs raise the possibility that RNAs directly influence chromatin remodeling. Therefore, we tested the effects of *Evf2* and *Dlx1UR* lncRNAs, *28S*, *pGEM* (artificial transcript), tRNA, and the highest-affinity binding ribohomopolymers polyG and polyA on BRG1-mediated ATPase activity and chromatin remodeling activity *in vitro* (Fig. 5). Sequence complex RNAs ($Evf2^{622}$, $28S^{630}$, $Dlx1UR^{534}$ and $pGEM^{535}$) are transcribed *in vitro* to generate similar length RNAs. With the exception of tRNA, the tested RNAs inhibit BRG1 ATPase and remodeling activities (Fig. 5).

Support that RNA-dependent inhibition of remodeling occurs through ATPase inhibition is based on the finding that IC_{50} (the concentration of RNA that inhibits ATPase or remodeling activity by 50%) values in the ATPase assay are lower than those observed in the remodeling assays (Fig. 5). The IC_{50} values for polyA RNA (1.50 µM) and polyG RNA (<0.21 µM) in ATPase inhibition are lower than the average IC_{50} for sequence complex RNAs (3.79 µM). The IC_{50} values for polyA RNA (1.84 µM) and polyG RNA (<0.21 µM) in remodeling inhibition are also lower than the average IC_{50} for sequence complex RNAs (13.66 µM). polyG RNA binds BRG1 with the highest affinity in both *Evf2*/REMSA competition (Fig. 4D) and polyU-agarose competition assays (Fig. 4G), supporting the contention that RNA-dependent inhibition of BRG1 ATPase and remodeling activity occurs through direct binding. Together, these data support RNA promiscuity in inhibiting the ATPase and remodeling activity of BRG1.

DISCUSSION

Histone-modifying enzymes and chromatin remodeling complexes constitute two major classes of proteins involved in regulating chromatin so that genes can be actively expressed or repressed. The SWI/SNF (yeast) and BAF (human) chromatin remodeling complexes recognize specific histone modifications and, in an ATP-dependent manner, reposition or eject nucleosomes (Workman and Kingston, 1992; Wang et al., 1996; Phelan et al., 1999; Clapier and Cairns, 2009; Kasten et al., 2011). lncRNAs are thought to repress gene expression through recruitment of histone-modifying enzymes (Rinn et al., 2007; Nagano et al., 2008; Pandey et al., 2008; Zhao et al., 2008), but a direct role for lncRNAs in chromatin remodeling has not been reported. However, experiments in *Arabidopsis* suggest that polV-produced lncRNAs interact with the lncRNA-binding protein ID2 and associate with SWI/SNF-related remodelers to silence gene expression through effects on nucleosome positioning (Zhu et al., 2013).

RNA binding properties of BRG

In this study, we propose that lncRNA-mediated transcriptional repression occurs through direct lncRNA-BRG1 binding and inhibition of BRG1 ATPase and chromatin remodeling activities (Fig. 5A,B and Fig. 6A,B). *In vitro* binding assays show that BRG1-RNA interactions are promiscuous and that the length of polyG ribohomopolymers is important (Fig. 4D-F). There are many RNA-binding proteins that exhibit non-specific or promiscuous RNA binding properties *in vitro*, but specific functional roles in the context of additional proteins or *in vivo*. Non-specific RNA binding has been described for factors involved in a wide range of RNA-dependent biological processes involving mRNA and microRNA processing, and promiscuous binding for lncRNA-polycomb repressor complex 2 (PRC2) interactions, where lncRNA repression is proposed to occur through a scanning model (Davidovich et al., 2013). In addition, early work on hnRNP-mediated RNA annealing activities and ribozyme catalysis led to the proposal that non-specific RNA-binding proteins may function as RNA chaperones, guiding RNA secondary or tertiary structures (Takagaki et al., 1992; Herschlag et al., 1994; Portman and Dreyfuss, 1994). It is of interest to note that preferential binding to specific ribohomopolymers is shared between BRG1/BAFs and

Development (2015) 142, 2641-2652 doi:10.1242/dev.126318

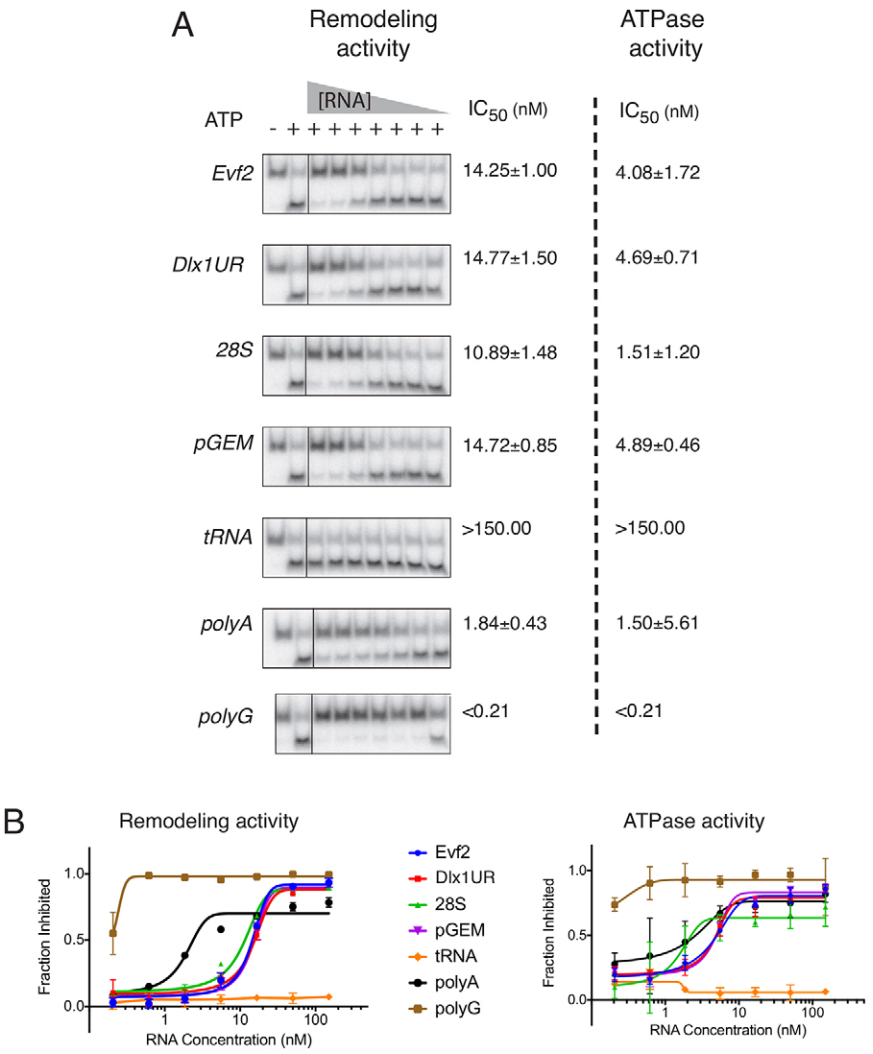

Fig. 5. RNA inhibits BRG1 chromatin remodeling activity through inhibition of ATPase activity. BRG1 ATPase activity and chromatin remodeling activity are measured in the presence of seven different RNAs: *Evf2*, *Dlx1UR*, *28S*, *pGEM*, tRNA, polyA, polyG. The IC_{50} (concentration of RNAs generating 50% inhibition of each activity) is indicated for each RNA. (A) BRG1 chromatin remodeling activity is assayed by nucleosome redistribution and restriction enzyme cleavage. Shown is acrylamide gel electrophoresis resolution of cut and uncut nucleosomes. BRG1 (100 nM) is incubated with trace nucleosomes (in 20 mM ATP, 3 mM $MgCl_2$) and decreasing concentrations of RNAs: 150, 50, 16.67, 5.56, 1.85, 0.62, 0.21 nM. BRG1 ATPase activity is determined by thin layer chromatography analysis of reactions in which BRG1 (100 nM) is incubated with saturating nucleosomes (in 2 μM ATP, 3 mM $MgCl_2$) and decreasing concentrations of RNAs as above. (B) Quantification of remodeling and ATPase assays; three independent experiments (error bars indicate s.e.m.).

members of the hnRNP family (Pinol-Roma et al., 1988) of RNA-binding proteins, some of which exhibit RNA chaperone activity. The known property of G-containing RNAs to form tetramers (Kim et al., 1991), combined with high-affinity polyG binding to BRG1 and BAFs (Fig. 4D,E), raises the possibility that RNA conformation might play a role in RNA-dependent inhibition of remodeling.

Model for an RNA-bound chromatin remodeler (R-CR) in negative-feedback inhibition

We initially set out to answer the following: how does RNA-dependent recruitment of activating factors result in transcriptional repression? Previous work showed that *Evf2* increases binding of both activators and repressors to the *Dlx5/6* enhancer (Bond et al., 2009; Berghoff et al., 2013), leading to the idea that *Evf2*-mediated transcriptional repression results from the cumulative effects of antagonism between DLX1/2 and MECP2. In this work, mass spectrometry analysis of immunoaffinity purified DLX complexes in $Evf2^{+/+}$ nuclear extracts (supplementary material Table S1) does not detect MECP2. This is consistent with a model in which DLX1/2 antagonism of MECP2 is competitive and occurs on mutually exclusive alleles (Bond et al., 2009; Berghoff et al., 2013). However, BRG1-RNA binding, and RNA-dependent direct inhibition of BRG1 ATPase and remodeling activity, support a role beyond that of mediating antagonism between transcription factors. Furthermore, *Evf2* not only increases BRG1 and DLX1 association at the *Dlx5/6* enhancers, but also increases histone acetylation (H3AcK9, H3AcK18, and H4AcK5 within *Dlx5/6* ei and eii; Fig. 3). Given that a role for H4 acetylation-mediated inhibition of ISWI remodeling activity has been reported (Shogren-Knaak et al., 2006), it is possible that, in the presence of *Evf2*, increased histone lysine acetylation might further stabilize BRG1/BAF association through bromodomain interactions (Hassan et al., 2002) and contribute to remodeling inhibition.

These data support a model of lncRNA-dependent transcriptional repression at enhancers, distinct from polycomb repressor complex recruitment (Fig. 6B). In this model, DLX1-BRG1-BAFs [the chromatin remodeler (CR)] form an active complex at *Dlx5/6* intergenic enhancers, activating adjacent gene expression (*Dlx5*, *Dlx6* and *Evf2*). This initial recruitment occurs independently of *Evf2*, as *Evf2* activation occurs after DLX1 binding. This is supported by genetic experiments in embryonic mouse brain: the requirement of BRG1 in *Dlx1* activation (Lessard et al., 2007) and the requirement of *Dlx1/2* in *Dlx5/6/Evf2* activation (Anderson et al., 1997b; Berghoff et al., 2013). Once *Evf2* expression is activated (Fig. 6B, red arrow), *Evf2* binds to BRG1/BAFs (R-CR), stabilizes the association with *Dlx5/6* ei and eii, and directly inhibits BRG1 remodeling activity through inhibition of ATPase activity. The R-CR converts an active enhancer bound by DLX1-BRG1-

Development (2015) 142, 2641-2652 doi:10.1242/dev.126318

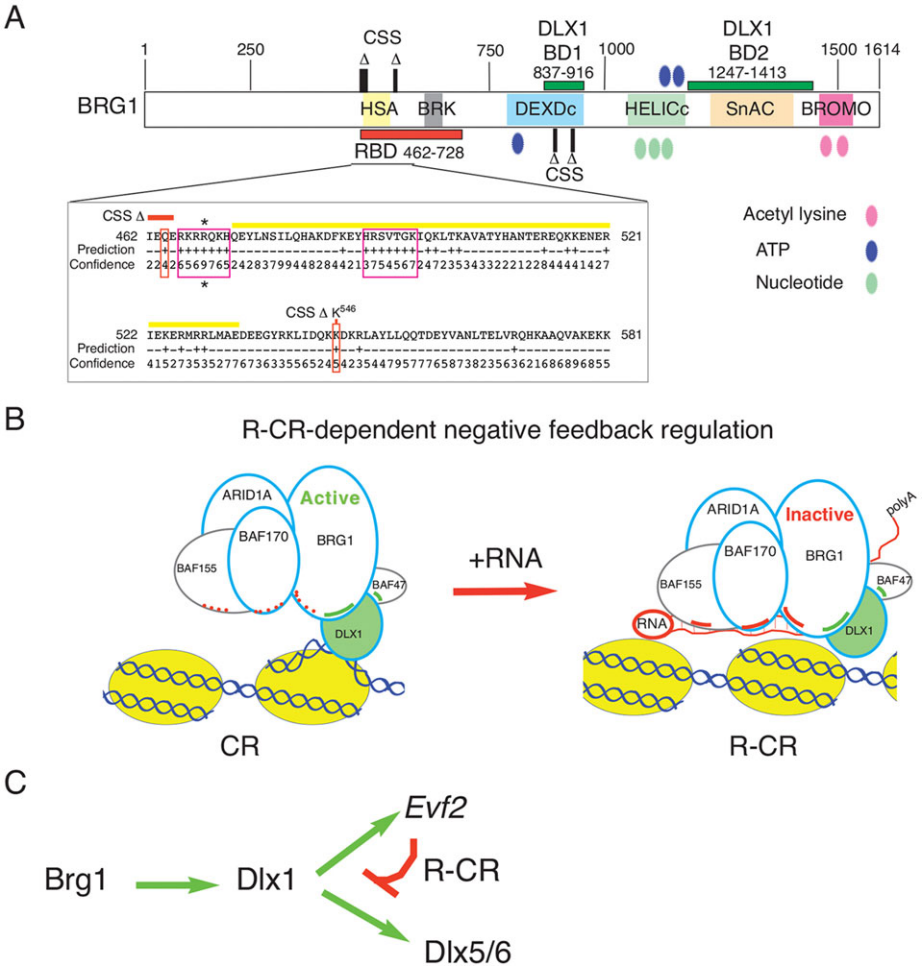

Fig. 6. A model for transcriptional repression through RNA-mediated inhibition of chromatin remodeling. (A) BRG1 deletion analysis identifies two BRG1 DLX1-binding domains: DLX1-BD1 at 837-916 and DLX1-BD2 at 1247-1413 (dark green). The proposed RNA-binding domain (RBD) is at 462-728 (red). Sequence is shown for the N-terminal region of the RBD (462-581, BRG1-N-RBD), which displays higher confidence levels of RNA binding, as predicted by the BINDN+ program (Wang and Brown, 2006), than the C-terminal RBD (582-728). BRG1-N-RBD contains two stretches of potential RNA-binding residues (boxed in pink), one of which overlaps with the HSA region (yellow). *R^{469} has the highest confidence level prediction (+9) for RNA binding. CSS Δ indicates mutations identified in Coffin–Siris syndrome (CSS) by human exome sequencing (Tsurusaki et al., 2012). The CSS mutations (boxed in red) that are predicted to be involved in RNA binding are Q^{464} and K^{546}. Two CSS mutations are found in BRG1 DLX1-BD1. (B) Model for RNA-dependent transcriptional repression. (Left) The *Dlx5/6* active enhancer is bound by the DLX1-active chromatin remodeler (CR). CR components identified by mass spectrometry in E13.5 GE extracts are outlined in blue [BRG1, BAF170, ARID1A (predicted)]; additional known CRs are outlined in gray (BAF155, BAF47). The DLX1 homeodomain transcription factor (green, outlined in blue) binds DNA in a sequence-specific manner and binds BRG1 and BAF47 proteins (green lines). Nucleosomes (yellow spheres) are wound by DNA. The red dotted lines represent BRG1, BAF170 and BAF155 RNA-binding potential. (Right) Once the enhancer is activated, *Evf2* (RNA, red) expression is activated. Sequence complex regions of the *Evf2* RNA bind BRG1, BAF170 and BAF155 (red lines), stabilizing R-CR complex association with DNA, inhibiting BRG1 ATPase activity and remodeling activity, and repressing enhancer activity. RNA transcription and/or RNA retention may contribute to dynamic and/or precise modulation of enhancer activity. BRG1 (Brahma-related gene 1) is the ATPase remodeling component of the CR; BAFs, BRG1-associated factors 170, 155, 47; DLX1 is a homeodomain-containing, sequence-specific DNA-binding protein that acts as a transcription factor crucial for *Evf2* and *Dlx5/6* expression. (C) In the embryonic brain, *Brg1* activates *Dlx1* gene expression. *Dlx1* activates *Dlx5*, *Dlx6* and *Evf2*. *Evf2* forms a complex with chromatin remodelers (R-CR), inhibits BRG1 remodeling activity, and attenuates *Dlx1* activation of *Dlx5/6*.

BAFs to an RNA-dependent repressed enhancer, supporting the idea that lncRNA activation functions in a negative-feedback mechanism to attenuate DLX1 activation.

In the proposed model, the lncRNA inhibits BRG1 ATPase and remodeling activity but the R-CR is retained at the enhancer, allowing subsequent gene reactivation. *Evf2* RNA loss does not change total H3 at the *Dlx5/6* ei, arguing against nucleosome ejection (Fig. 3E). It will be important to determine whether RNA binding is actually dynamic (CR↔R-CR) or is an endpoint, as shown in the model (Fig. 6B,C). A dynamic model is attractive in that RNA-bound activators are temporarily stabilized in order to achieve precise or rapid regulation. However, other possibilities that could achieve precise gene regulation include sequestration of positive factors, allele-specific effects, and transient and/or indirect effects of the RNA. The heterogeneity of individual profiles in the relationship between *Evf2* nuclear clouds and BRG1 enrichment supports a complex mechanism, requiring future experiments to distinguish between dynamic, sequestration and allele-specific roles of the R-CR.

A recent report shows that the *Myheart* (*Mhrt*; myosin heavy chain-associated RNA transcript) lncRNA binds to BRG1 through the helicase domain, repressing gene expression through direct competition of BRG1-DNA binding (Han et al., 2014). Given that the BRG1 RBD defined in our work is distinct from that of MHRT

Development (2015) 142, 2641-2652 doi:10.1242/dev.126318

(Fig. 6A), it will be important to determine the relative contributions of promiscuous RNA binding/remodeling inhibition and direct RNA-DNA competition in BRG1-lncRNA-mediated transcriptional repression. In addition to BRG1-lncRNA interactions in chromatin, SWI/SNF complexes have recently been shown to function in the assembly of nuclear bodies containing the lncRNA *NEAT1* (Kawaguchi et al., 2015), thereby expanding the role of BRG1-lncRNA interactions in the nucleus.

Although direct interactions between *Evf2*, DLX1 and SWI/SNF, and binding of BRG1-DLX1 to *Dlx5/6* enhancers, support a direct role of *Evf2* RNA in BRG1 transcriptional regulation, it is also possible that the *Evf2* RNA cloud plays a role as a 'sink' for proteins or other RNAs. Although it remains to be determined how many proteins, in addition to BRG1 and DLX, localize within the *Evf2* RNA cloud, mass spectrometry of DLX-bound proteins predicts the presence of a large number of proteins with diverse functions. In light of SWI/SNF regulation of nuclear body assembly (Kawaguchi et al., 2015), it will be important to determine whether BRG1 and/or other DLX-bound proteins identified by mass spectrometry play a role in *Evf2* RNA cloud formation, and whether *Evf2* directly or indirectly affects the subnuclear organization/sequestering of factors involved in transcriptional regulation.

Biological significance of BRG1 RNA-binding and DLX1-binding domains

Several lines of evidence support the biological significance of *Evf2* and DLX1 interactions during embryonic forebrain development. DLX1/2 regulate *Dlx5/6* gene expression, and belong to a family of homeodomain transcription factors known for their roles in interneuron migration and differentiation (Panganiban and Rubenstein, 2002). Mice lacking *Dlx1*, *2*, *5* and/or *6*, either alone or in combination, exhibit a range of neuronal, craniofacial and limb defects (Anderson et al., 1997a,b; Depew et al., 1999; Pleasure et al., 2000; Merlo et al., 2002; Robledo et al., 2002; Cobos et al., 2005; Wang et al., 2010). In accordance with its role in regulating *Dlx5/6* genes, mice lacking *Evf2* display synaptic defects in the adult hippocampus (Bond et al., 2009).

The biological significance of CRs is highlighted by the recent identification of multiple CR mutations in human patients with autism, autism spectrum disorders (ASDs), schizophrenia and intellectual disability (reviewed by Staahl and Crabtree, 2013; Vogel-Ciernia and Wood, 2014). CSS is characterized by growth deficiency, intellectual disability, microcephaly, coarse facial features and nail defects; 20/23 CSS patients were reported to have a mutation in one of six SWI/SNF subunits, including BRG1 (Tsurusaki et al., 2012, 2014). Two BRG1 CSS deletion/mutations map within the N-terminal RBD domain (red boxes, Fig. 6A), while another two are in DLX1-binding domain 1 (837-916), raising the possibility that R-CR interactions might be involved (Fig. 6A). It is interesting that previous reports have linked disruption of *Dlx5/6*-dependent control of GABAergic interneuron development/function with autism. Loss of MECP2 in *Dlx5/6*-expressing GABAergic interneurons results in many behaviors associated with Rett syndrome, an ASD in humans (Nan et al., 1997; Chao et al., 2010). Loss of MECP2 increases *Evf2* and *Dlx5* expression in E13.5 GE (Berghoff et al., 2013) and *Dlx5/6* expression in postnatal cortex (Horike et al., 2005). Loss of *Evf2* destabilizes MECP2 binding to *Dlx5/6* ei and eii, also resulting in increased *Dlx5* and *Dlx6* expression in E13.5 GE (Bond et al., 2009). *Dlx1*/2 antagonize MECP2 repression of *Dlx5* (Berghoff et al., 2013). A *Dlx5/6* ei SNP that disrupts DLX1/2 binding was identified in an autistic proband (Poitras et al., 2010). Given the global DNA-binding properties of MECP2, it has been difficult to envision how this may cause such specific neurological phenotypes, as in Rett syndrome. A similar problem stems from CR mutations, as CRs also control transcription globally. Together, these data raise an important question as to whether R-CRs provide the precise gene regulation necessary for higher order brain function and, when disrupted (as in MECP2 and CR mutations), how they might cause the subtle defects found in specific human neurological disorders.

MATERIALS AND METHODS

Primer and sequence data

Details of primers and sequence information for all RNAs are provided in the supplementary material Methods.

RNP isolation and protein identification

DLX immunoaffinity purification of complexes was performed from nuclear extracts (Dignam et al., 1983) using E13.5 GE of *Evf2*$^{+/+}$ or *Evf2*$^{TS/TS}$ mice (Bond et al., 2009) or Swiss-Webster timed pregnant dams (Taconic) and anti-DLX antibody (Feng et al., 2006). Differential mass spectrometry and multidimensional protein identification technology were performed on DLX immunoaffinity purified complexes as previously described (Washburn et al., 2001). Supplementary material Table S1 lists mass spectrometry proteins identified in DLX-bound complexes from *Evf2*$^{+/+}$ and *Evf2*$^{TS/TS}$ nuclear extract lysates. Raw data from mass spectrometry analysis can be accessed at: http://fields.scripps.edu/published/evf/. The mass spectrometry data have been submitted to Dryad and can be accessed under the doi: 10.5061/dryad.82gn0. The institutional IACUC committee approved all animal procedures.

Fluorescent *in situ* hybridization and immunohistochemistry colabeling (FISH-immuno)

FISH on E13.5 GE sections was performed using digoxigenin antisense *Evf2* RNA probe as previously described (Feng et al., 2006) and 1:500 dilution of rabbit polyclonal anti-BRG1 (Wang et al., 1996), with tyramide amplification (Invitrogen). Details of *Evf2* RNA and BRG1 protein colocalization are included in the supplementary material Methods.

Chromatin immunoprecipitation (ChIP)

E13.5 GE chromatin (25 µg) was diluted 1:10 in RIPA buffer (10 mM Tris pH 7.6, 1 mM EDTA, 0.1% SDS, 0.1% sodium deoxycholate, 1% Triton X-100) with protease inhibitors (Roche), precleared by incubating with protein G agarose (Roche), and incubated with 2 or 5 µg ChIP-verified antibodies overnight at 4°C. The immunoprecipitated DNA was purified using the Qiaquick PCR Purification Kit (Qiagen). Immunoprecipitated DNA diluted 1:20 (in double-distilled water), primers, and Perfecta SYBR Green Fast Mix (Quanta Biosciences) was combined to 20 µl total reaction volume in a MicroAmp Fast Optical 96-well Reaction Plate (Life Technologies). Quantification of the immunoprecipitated material was performed in the Fast 7500 Real-Time PCR System (Life Technologies). For ChIP/reChIP, the ChIP protocol described above was used to perform anti-DLX ChIP, followed by elution and re-immunoprecipitation with anti-BRG1, anti-lamin B1 or anti-IgG as described (Truax and Greer, 2012). Percent input values obtained for IgG were subtracted from anti-BRG1 and anti-lamin B1 values. Statistical analysis employed an unpaired Student's *t*-test with equal variance. A detailed protocol for ChIP/reCHIP is included in the supplementary material Methods.

RNP interactions

The REMSA assembly reactions were carried out as described (Thomson et al., 1999) with several modifications. The RNA probe was labeled using near-infrared (NIR) *in vitro* transcription as described (Kohn et al., 2010). Flag-tagged BRG1 and BAF47, BAF155 and BAF170 proteins were purified from SF9 insect cells according to the Invitrogen Bac-to-Bac baculovirus expression system. The recombinant proteins were incubated with 0.15 pmoles *Evf2* NIR-labeled probe in 10 µl reactions for 30 min at room temperature. For all competition experiments, protein and competitor RNA were pre-incubated for 10 min at room temperature before adding

probe. *Evf2*, *28S*, *pGEM* and *Dlx1UR* competitor RNAs were generated by *in vitro* transcription as described in the supplementary material Methods. The ribohomopolymers were obtained from Sigma (polyA, polyG) or Midland (polyC, polyU). The 19 nt RNA oligos were obtained from IDT DNA. 5 µg tRNA and 0.5 µl RNasin (Promega) were included in all the REMSA reactions. Pre-electrophoresis of 4% native polyacrylamide gels was performed for 20 min, REMSA reactions loaded and electrophoresed at 200 V for 40 min, and data visualized in the Odyssey Infrared Imager (LI-COR Biosciences). Comparisons of BRG1 binding to different ribohomopolymers were performed using a polyU-agarose binding assay, in which 8 picomoles of BRG1 was preincubated with the different soluble ribohomopolymers mentioned above. Further details of REMSAs and polyU-agarose binding assays are provided in the supplementary material Methods and Table S3.

BRG1 ATPase and remodeling assays

For protein purification and nucleosome assembly, Flag-epitope BRG1 and BRG1 mutants were purified from SF9 cells using baculovirus expression as previously described (Phelan et al., 1999). Recombinant histones were purified and reconstituted into octamers as described previously (Luger et al., 1999). Mononucleosomes were assembled onto a 237-bp DNA fragment containing a central 601 positioning sequence that had been modified to contain an internal *Pst*I cleavage site. Conditions for RNA inhibition of BRG1 ATPase and remodeling activities are detailed in the supplementary material Methods and Table S3.

Acknowledgements

We thank Dr Weidong Wang (NIH) for the kind gift of rabbit anti-BRG1 antibody (multiple shipments); Dr Robin Park (Scripps) for the Venn diagram in Fig. 1; and Dr Michael VanGompel (present address UC Davis) for help with screening the UCR database (supplementary material Fig. S2).

Competing interests

The authors declare no competing or financial interests.

Author contributions

I.C. performed experiments (Figs 1, 3 and 4; supplementary data) and helped in manuscript preparation. D.E.L. established conditions for isolating embryonic brain RNPs, and RNA protein REMSAs. J.C. and R.E.K. contributed the BRG1 ATPase and remodeling experiments (Fig. 5). H.L. performed the BRG1-DLX1 direct interaction experiments (Fig. 2). K.S. performed reChIP experiments (Fig. 1). S.C. performed experiments in Figs 1 and 3. B.S.C. performed the screen of ucRNAs in E13.5 GE (Fig. 3; supplementary data). J.T. and J.R.Y. contributed mass spectroscopy results (Fig. 1; supplementary data). J.D.K. conceived experiments, proposed the model (Fig. 6) and prepared the manuscript.

Funding

This work was initially funded by the American Reinvestment and Recovery Act and the National Institute of Child Health and Human Development (NICHD) [R01HD056504 (2009-2011) to J.D.K.]; and presently by the National Institute of Mental Health (NIMH) [R01MH094653 to J.D.K.]; and the National Institute of General Medical Sciences (NIGMS) [5R37 GM048405-23 to R.E.K. and P41 GM103533 to J.R.Y.]. Deposited in PMC for release after 12 months.

Supplementary material

Supplementary material available online at
http://dev.biologists.org/lookup/suppl/doi:10.1242/dev.126318/-/DC1

References

Anderson, S. A., Eisenstat, D. D., Shi, L. and Rubenstein, J. L. R. (1997a). Interneuron migration from basal forebrain to neocortex: dependence on Dlx genes. *Science* **278**, 474-476.

Anderson, S. A., Qiu, M., Bulfone, A., Eisenstat, D. D., Meneses, J., Pedersen, R. and Rubenstein, J. L. R. (1997b). Mutations of the homeobox genes Dlx-1 and Dlx-2 disrupt the striatal subventricular zone and differentiation of late born striatal neurons. *Neuron* **19**, 27-37.

Berghoff, E. G., Clark, M. F., Chen, S., Cajigas, I., Leib, D. E. and Kohtz, J. D. (2013). Evf2 (Dlx6as) lncRNA regulates ultraconserved enhancer methylation and the differential transcriptional control of adjacent genes. *Development* **140**, 4407-4416.

Bond, A. M., VanGompel, M. J. W., Sametsky, E. A., Clark, M. F., Savage, J. C., Disterhoft, J. F. and Kohtz, J. D. (2009). Balanced gene regulation by an embryonic brain ncRNA is critical for adult hippocampal GABA circuitry. *Nat. Neurosci.* **12**, 1020-1027.

Brockdorff, N. (2011). Chromosome silencing mechanisms in X-chromosome inactivation: unknown unknowns. *Development* **138**, 5057-5065.

Calin, G. A., Liu, C.-G., Ferracin, M., Hyslop, T., Spizzo, R., Sevignani, C., Fabbri, M., Cimmino, A., Lee, E. J., Wojcik, S. E. et al. (2007). Ultraconserved regions encoding ncRNAs are altered in human leukemias and carcinomas. *Cancer Cell* **12**, 215-229.

Chao, H.-T., Chen, H., Samaco, R. C., Xue, M., Chahrour, M., Yoo, J., Neul, J. L., Gong, S., Lu, H.-C., Heintz, N. et al. (2010). Dysfunction in GABA signalling mediates autism-like stereotypies and Rett syndrome phenotypes. *Nature* **468**, 263-269.

Clapier, C. R. and Cairns, B. R. (2009). The biology of chromatin remodeling complexes. *Annu. Rev. Biochem.* **78**, 273-304.

Cobos, I., Calcagnotto, M. E., Vilaythong, A. J., Thwin, M. T., Noebels, J. L., Baraban, S. C. and Rubenstein, J. L. R. (2005). Mice lacking Dlx1 show subtype-specific loss of interneurons, reduced inhibition and epilepsy. *Nat. Neurosci.* **8**, 1059-1068.

Davidovich, C., Zheng, L., Goodrich, K. J. and Cech, T. R. (2013). Promiscuous RNA binding by Polycomb repressive complex 2. *Nat. Struct. Mol. Biol.* **20**, 1250-1257.

Depew, M. J., Liu, J. K., Long, J. E., Presley, R., Meneses, J. J., Pedersen, R. A. and Rubenstein, J. L. (1999). Dlx5 regulates regional development of the branchial arches and sensory capsules. *Development* **126**, 3831-3846.

Dignam, J. D., Lebovitz, R. M. and Roeder, R. G. (1983). Accurate transcription initiation by RNA polymerase II in a soluble extract from isolated mammalian nuclei. *Nucleic Acids Res.* **11**, 1475-1489.

Feng, J., White, B., Tyurina, O. V., Guner, B., Larson, T., Lee, H. Y., Karlstrom, R. O. and Kohtz, J. D. (2004). Synergistic and antagonistic roles of the Sonic hedgehog N- and C-terminal lipids. *Development* **131**, 4357-4370.

Feng, J., Bi, C., Clark, B. S., Mady, R., Shah, P. and Kohtz, J. D. (2006). The Evf-2 noncoding RNA is transcribed from the Dlx-5/6 ultraconserved region and functions as a Dlx-2 transcriptional coactivator. *Genes Dev.* **20**, 1470-1484.

Gabory, A., Ripoche, M.-A., Le Digarcher, A., Watrin, F., Ziyyat, A., Forne, T., Jammes, H., Ainscough, J. F. X., Surani, M. A., Journot, L. et al. (2009). H19 acts as a trans regulator of the imprinted gene network controlling growth in mice. *Development* **136**, 3413-3421.

Geisler, S. and Coller, J. (2013). RNA in unexpected places: long non-coding RNA functions in diverse cellular contexts. *Nat. Rev. Mol. Cell Biol.* **14**, 699-712.

Gomez, J. A., Wapinski, O. L., Yang, Y. W., Bureau, J.-F., Gopinath, S., Monack, D. M., Chang, H. Y., Brahic, M. and Kirkegaard, K. (2013). The NeST long ncRNA controls microbial susceptibility and epigenetic activation of the interferon-gamma locus. *Cell* **152**, 743-754.

Gutschner, T., Hammerle, M., Eissmann, M., Hsu, J., Kim, Y., Hung, G., Revenko, A., Arun, G., Stentrup, M., Gross, M. et al. (2013). The noncoding RNA MALAT1 is a critical regulator of the metastasis phenotype of lung cancer cells. *Cancer Res.* **73**, 1180-1189.

Han, P., Li, W., Lin, C.-H., Yang, J., Shang, C., Nurnberg, S. T., Jin, K. K., Xu, W., Lin, C.-Y., Lin, C.-J. et al. (2014). A long noncoding RNA protects the heart from pathological hypertrophy. *Nature* **514**, 102-106.

Hassan, A. H., Prochasson, P., Neely, K. E., Galasinski, S. C., Chandy, M., Carrozza, M. J. and Workman, J. L. (2002). Function and selectivity of bromodomains in anchoring chromatin-modifying complexes to promoter nucleosomes. *Cell* **111**, 369-379.

Herschlag, D., Khosla, M., Tsuchihashi, Z. and Karpel, R. L. (1994). An RNA chaperone activity of non-specific RNA binding proteins in hammerhead ribozyme catalysis. *EMBO J.* **13**, 2913-2924.

Horike, S., Cai, S., Miyano, M., Cheng, J. F. and Kohwi-Shigematsu, T. (2005). Loss of silent-chromatin looping and impaired imprinting of DLX5 in Rett syndrome. *Nat. Genet.* **37**, 31-40.

Kasten, M. M., Clapier, C. R. and Cairns, B. R. (2011). SnapShot: chromatin remodeling: SWI/SNF. *Cell* **144**, 310-310.e311.

Kawaguchi, T., Tanigawa, A., Naganuma, T., Ohkawa, Y., Souquere, S., Pierron, G. and Hirose, T. (2015). SWI/SNF chromatin-remodeling complexes function in noncoding RNA-dependent assembly of nuclear bodies. *Proc. Natl. Acad. Sci. USA* **112**, 4304-4309.

Kim, J., Cheong, C. and Moore, P. B. (1991). Tetramerization of an RNA oligonucleotide containing a GGGG sequence. *Nature* **351**, 331-332.

Kohn, M., Lederer, M., Wachter, K. and Huttelmaier, S. (2010). Near-infrared (NIR) dye-labeled RNAs identify binding of ZBP1 to the noncoding Y3-RNA. *RNA* **16**, 1420-1428.

Kohtz, J. D. and Berghoff, E. G. (2010). Regulatory long non-coding RNAs and neuronal disorders. *Physiol. Behav.* **100**, 250-254.

Kohtz, J. D., Baker, D. P., Corte, G. and Fishell, G. (1998). Regionalization within the mammalian telencephalon is mediated by changes in responsiveness to Sonic Hedgehog. *Development* **125**, 5079-5089.

Kohtz, J. D., Lee, H. Y., Gaiano, N., Segal, J., Ng, E., Larson, T., Baker, D. P., Garber, E. A., Williams, K. P. and Fishell, G. (2001). N-terminal fatty-acylation of sonic hedgehog enhances the induction of rodent ventral forebrain neurons. *Development* **128**, 2351-2363.

Lanz, R. B., McKenna, N. J., Onate, S. A., Albrecht, U., Wong, J., Tsai, S. Y., Tsai, M.-J. and O'Malley, B. W. (1999). A steroid receptor coactivator, SRA, functions as an RNA and is present in an SRC-1 complex. *Cell* **97**, 17-27.

Lessard, J., Wu, J. I., Ranish, J. A., Wan, M., Winslow, M. M., Staahl, B. T., Wu, H., Aebersold, R., Graef, I. A. and Crabtree, G. R. (2007). An essential switch in subunit composition of a chromatin remodeling complex during neural development. *Neuron* **55**, 201-215.

Luger, K., Rechsteiner, T. J. and Richmond, T. J. (1999). Expression and purification of recombinant histones and nucleosome reconstitution. *Methods Mol. Biol.* **119**, 1-16.

Marigo, V., Davey, R. A., Zuo, Y., Cunningham, J. M. and Tabin, C. J. (1996). Biochemical evidence that patched is the Hedgehog receptor. *Nature* **384**, 176-179.

Merlo, G. R., Paleari, L., Mantero, S., Genova, F., Beverdam, A., Palmisano, G. L., Barbieri, O. and Levi, G. (2002). Mouse model of split hand/foot malformation type I. *Genesis* **33**, 97-101.

Nagano, T., Mitchell, J. A., Sanz, L. A., Pauler, F. M., Ferguson-Smith, A. C., Feil, R. and Fraser, P. (2008). The Air noncoding RNA epigenetically silences transcription by targeting G9a to chromatin. *Science* **322**, 1717-1720.

Nan, X., Campoy, F. J. and Bird, A. (1997). MeCP2 is a transcriptional repressor with abundant binding sites in genomic chromatin. *Cell* **88**, 471-481.

Ørom, U. A., Derrien, T., Beringer, M., Gumireddy, K., Gardini, A., Bussotti, G., Lai, F., Zytnicki, M., Notredame, C., Huang, Q. et al. (2010). Long noncoding RNAs with enhancer-like function in human cells. *Cell* **143**, 46-58.

Pandey, R. R., Mondal, T., Mohammad, F., Enroth, S., Redrup, L., Komorowski, J., Nagano, T., Mancini-DiNardo, D. and Kanduri, C. (2008). Kcnq1ot1 antisense noncoding RNA mediates lineage-specific transcriptional silencing through chromatin-level regulation. *Mol. Cell* **32**, 232-246.

Panganiban, G. and Rubenstein, J. L. (2002). Developmental functions of the Distal-less/Dlx homeobox genes. *Development* **129**, 4371-4386.

Phelan, M. L., Sif, S., Narlikar, G. J. and Kingston, R. E. (1999). Reconstitution of a core chromatin remodeling complex from SWI/SNF subunits. *Mol. Cell* **3**, 247-253.

Pinol-Roma, S., Choi, Y. D., Matunis, M. J. and Dreyfuss, G. (1988). Immunopurification of heterogeneous nuclear ribonucleoprotein particles reveals an assortment of RNA-binding proteins. *Genes Dev.* **2**, 215-227.

Pleasure, S. J., Anderson, S., Hevner, R., Bagri, A., Marin, O., Lowenstein, D. H. and Rubenstein, J. L. R. (2000). Cell migration from the ganglionic eminences is required for the development of hippocampal GABAergic interneurons. *Neuron* **28**, 727-740.

Poitras, L., Yu, M., Lesage-Pelletier, C., MacDonald, R. B., Gagne, J.-P., Hatch, G., Kelly, I., Hamilton, S. P., Rubenstein, J. L. R., Poirier, G. G. et al. (2010). An SNP in an ultraconserved regulatory element affects Dlx5/Dlx6 regulation in the forebrain. *Development* **137**, 3089-3097.

Portman, D. S. and Dreyfuss, G. (1994). RNA annealing activities in HeLa nuclei. *EMBO J.* **13**, 213-221.

Rapicavoli, N. A., Poth, E. M., Zhu, H. and Blackshaw, S. (2011). The long noncoding RNA Six3OS acts in trans to regulate retinal development by modulating Six3 activity. *Neural Dev.* **6**, 32.

Redrup, L., Branco, M. R., Perdeaux, E. R., Krueger, C., Lewis, A., Santos, F., Nagano, T., Cobb, B. S., Fraser, P. and Reik, W. (2009). The long noncoding RNA Kcnq1ot1 organises a lineage-specific nuclear domain for epigenetic gene silencing. *Development* **136**, 525-530.

Rinn, J. L., Kertesz, M., Wang, J. K., Squazzo, S. L., Xu, X., Brugmann, S. A., Goodnough, L. H., Helms, J. A., Farnham, P. J., Segal, E. et al. (2007). Functional demarcation of active and silent chromatin domains in human HOX loci by noncoding RNAs. *Cell* **129**, 1311-1323.

Robledo, R. F., Rajan, L., Li, X. and Lufkin, T. (2002). The Dlx5 and Dlx6 homeobox genes are essential for craniofacial, axial, and appendicular skeletal development. *Genes Dev.* **16**, 1089-1101.

Sen, P., Vivas, P., Dechassa, M. L., Mooney, A. M., Poirier, M. G. and Bartholomew, B. (2013). The SnAC domain of SWI/SNF is a histone anchor required for remodeling. *Mol. Cell. Biol.* **33**, 360-370.

Shogren-Knaak, M., Ishii, H., Sun, J.-M., Pazin, M. J., Davie, J. R. and Peterson, C. L. (2006). Histone H4-K16 acetylation controls chromatin structure and protein interactions. *Science* **311**, 844-847.

Staahl, B. T. and Crabtree, G. R. (2013). Creating a neural specific chromatin landscape by npBAF and nBAF complexes. *Curr. Opin. Neurobiol.* **23**, 903-913.

Stone, D. M., Hynes, M., Armanini, M., Swanson, T. A., Gu, Q., Johnson, R. L., Scott, M. P., Pennica, D., Goddard, A., Phillips, H. et al. (1996). The tumour-suppressor gene patched encodes a candidate receptor for Sonic hedgehog. *Nature* **384**, 129-134.

Takagaki, Y., MacDonald, C. C., Shenk, T. and Manley, J. L. (1992). The human 64-kDa polyadenylylation factor contains a ribonucleoprotein-type RNA binding domain and unusual auxiliary motifs. *Proc. Natl. Acad. Sci. USA* **89**, 1403-1407.

Thomson, A. M., Rogers, J. T., Walker, C. E., Staton, J. M. and Leedman, P. J. (1999). Optimized RNA gel-shift and UV cross-linking assays for characterization of cytoplasmic RNA-protein interactions. *BioTechniques* **27**, 1032-1039, 1042.

Truax, A. D. and Greer, S. F. (2012). ChIP and re-ChIP assays: investigating interactions between regulatory proteins, histone modifications, and the DNA sequences to which they bind. *Meth. Mol. Biol.* **809**, 175-188.

Tsurusaki, Y., Okamoto, N., Ohashi, H., Kosho, T., Imai, Y., Hibi-Ko, Y., Kaname, T., Naritomi, K., Kawame, H., Wakui, K. et al. (2012). Mutations affecting components of the SWI/SNF complex cause Coffin-Siris syndrome. *Nat. Genet.* **44**, 376-378.

Tsurusaki, Y., Okamoto, N., Ohashi, H., Mizuno, S., Matsumoto, N., Makita, Y., Fukuda, M., Isidor, B., Perrier, J., Aggarwal, S. et al. (2014). Coffin-Siris syndrome is a SWI/SNF complex disorder. *Clin. Genet.* **85**, 548-554.

Vogel-Ciernia, A. and Wood, M. A. (2014). Neuron-specific chromatin remodeling: a missing link in epigenetic mechanisms underlying synaptic plasticity, memory, and intellectual disability disorders. *Neuropharmacology* **80**, 18-27.

Wang, L. and Brown, S. J. (2006). BindN: a web-based tool for efficient prediction of DNA and RNA binding sites in amino acid sequences. *Nucleic Acids Res.* **34**, W243-W248.

Wang, W., Cote, J., Xue, Y., Zhou, S., Khavari, P. A., Biggar, S. R., Muchardt, C., Kalpana, G. V., Goff, S. P., Yaniv, M. et al. (1996). Purification and biochemical heterogeneity of the mammalian SWI-SNF complex. *EMBO J.* **15**, 5370-5382.

Wang, Y., Dye, C. A., Sohal, V., Long, J. E., Estrada, R. C., Roztocil, T., Lufkin, T., Deisseroth, K., Baraban, S. C. and Rubenstein, J. L. R. (2010). Dlx5 and Dlx6 regulate the development of parvalbumin-expressing cortical interneurons. *J. Neurosci.* **30**, 5334-5345.

Washburn, M. P., Wolters, D. and Yates, J. R.III. (2001). Large-scale analysis of the yeast proteome by multidimensional protein identification technology. *Nat. Biotechnol.* **19**, 242-247.

Whitehouse, I., Flaus, A., Cairns, B. R., White, M. F., Workman, J. L. and Owen-Hughes, T. (1999). Nucleosome mobilization catalysed by the yeast SWI/SNF complex. *Nature* **400**, 784-787.

Woolfe, A., Goodson, M., Goode, D. K., Snell, P., McEwen, G. K., Vavouri, T., Smith, S. F., North, P., Callaway, H., Kelly, K. et al. (2005). Highly conserved non-coding sequences are associated with vertebrate development. *PLoS Biol.* **3**, e7.

Workman, J. L. and Kingston, R. E. (1992). Nucleosome core displacement in vitro via a metastable transcription factor-nucleosome complex. *Science* **258**, 1780-1784.

Yang, L., Froberg, J. E. and Lee, J. T. (2014). Long noncoding RNAs: fresh perspectives into the RNA world. *Trends Biochem. Sci.* **39**, 35-43.

Yelin, R., Dahary, D., Sorek, R., Levanon, E. Y., Goldstein, O., Shoshan, A., Diber, A., Biton, S., Tamir, Y., Khosravi, R. et al. (2003). Widespread occurrence of antisense transcription in the human genome. *Nat. Biotechnol.* **21**, 379-386.

Yoo, A. S. and Crabtree, G. R. (2009). ATP-dependent chromatin remodeling in neural development. *Curr. Opin. Neurobiol.* **19**, 120-126.

Zerucha, T., Stuhmer, T., Hatch, G., Park, B. K., Long, Q., Yu, G., Gambarotta, A., Schultz, J. R., Rubenstein, J. L. and Ekker, M. (2000). A highly conserved enhancer in the Dlx5/Dlx6 intergenic region is the site of cross-regulatory interactions between Dlx genes in the embryonic forebrain. *J. Neurosci.* **20**, 709-721.

Zhao, J., Sun, B. K., Erwin, J. A., Song, J.-J. and Lee, J. T. (2008). Polycomb proteins targeted by a short repeat RNA to the mouse X chromosome. *Science* **322**, 750-756.

Zhao, X., Tang, Z., Zhang, H., Atianjoh, F. E., Zhao, J.-Y., Liang, L., Wang, W., Guan, X., Kao, S.-C., Tiwari, V. et al. (2013). A long noncoding RNA contributes to neuropathic pain by silencing Kcna2 in primary afferent neurons. *Nat. Neurosci.* **16**, 1024-1031.

Zhu, Y., Rowley, M. J., Böhmdorfer, G. and Wierzbicki, A. T. (2013). A SWI/SNF chromatin-remodeling complex acts in noncoding RNA-mediated transcriptional silencing. *Mol. Cell* **49**, 298-309.